

Three-Dimensional Simulation of Flow-Field around a Flapping Foil using Immersed Boundary Solvers of OpenFOAM

Chandan Bose¹, Sayan Gupta² & Sunetra Sarkar²

1. University of Liege, Liege 4000, Belgium, cb.ju.1991@gmail.com

2. Indian Institute of Technology Madras, Chennai 600036, India, gupta.sayan@gmail.com,
sunetra.sarkar@gmail.com

Biologically inspired micro-aerial vehicles (MAVs) and autonomous underwater vehicles (AUVs) have sparked significant research attention in unsteady aero and hydrodynamics of flapping wings and fins [1, 2]. Most of these studies focused on two-dimensional (2D) canonical flapping models. The 2D assumption is valid for some species of birds and insects with relatively high-AR wings, such that the effects of the span-wise variability in the flow-field can be neglected. The three-dimensional (3D) effects become predominant for insects and fishes, possessing low-AR (< 5) wings and fins to facilitate high agility during their locomotion [3, 4]. Nature-inspired man-made flapping devices require low-AR wings/fins for agile motion in complex environments. Therefore, a thorough understanding of the 3D flow-field of low-AR flapping wings/fins is crucial for their efficient design.

The present study investigates the 3D wake past a finite-span plunging wing at Reynolds number (Re) of 250. The focus is on revealing new transitional wake dynamics behind a low-AR flapping wing in order to understand the interactions among leading-edge, trailing-edge, and tip vortices (LEV, TEV and TiVs). A discrete direct-forcing immersed boundary method (IBM) is employed to solve the 3D incompressible Navier-Stokes (N-S) equation. Kinematic parameters, particularly amplitude and frequency of the plunge motion, are found to have significant effects on the transition in the three-dimensional wake topology. The underlying vortex shedding mechanisms are unraveled with the aid of the Q-criterion iso-surfaces and streamlines. A transition from periodic bifurcated wake to completely aperiodic wake is observed with the increase in Strouhal number. The formation, growth, and separation of the 3D leading-edge vortex and its role behind the loss of periodicity of the wake are presented.

Computational Methodology:

An IBM-based finite volume N-S solver, available in an extended version of open-source libraries of OpenFOAM (foam-extend 3.2) [5], is used to simulate the 3D unsteady flow-field around a low-AR flapping wing. IBM is chosen for the simulations over boundary-fitted methods, such as the arbitrary Lagrangian-Eulerian (ALE) approach as it significantly reduces the computational cost of the 3D fluid dynamic simulations involving flow interactions with

moving boundaries. The IBM solver, used [6], follows a discrete-direct forcing approach. It requires a fixed Eulerian mesh on which the N-S equations are discretized and an immersed boundary (IB) surface (stationary or moving) corresponding to the obstruction in the flow, the location of which is traced by Lagrangian markers. The IB surface is introduced as a FTR (FOAM tri-surface) format derived from a STL (STereo-Lithography) file having the triangulated IB grid data. At every time step, the computational grid points are classified into fluid cells, solid cells, and IB cells based on the location of the solid boundary surface intersecting the fluid domain. The cells inside the IB surface are conventionally tagged as solid cells that do not contribute to the solution. Immersed boundary cells are identified as the fluid cells cut by the immersed boundary and have at least one face outside the IB surface. The rest of the outside cells are tagged as fluid cells where the N-S equation is solved without any modification. For the discrete-direct approach, the imposition of immersed boundary conditions is achieved through modifying the discretized governing equations near the IB to directly impose the boundary conditions on IB cells. In contrast with other indirect imposition approaches, there is no forcing term introduced into the governing equations either in continuous or in discretized form. Values of dependent variables in the IB cell centers are calculated at each time step by interpolation using neighboring cells' values and the boundary condition at the corresponding IB points. Appropriate boundary conditions are enforced on the IB points using a weighted least squares (WLS) interpolation to ensure a sharp representation of the structural boundary eliminating smearing. Global mass conservation is satisfied by scaling the fluxes through the face-cage enclosing the immersed boundary.

Computational Domain, Mesh and Validation:

A finite-span NACA0012 wing is chosen for the present simulations. The wing-span (S) is considered to be two times the chord-length (c). A rectangular computational domain of size $26c \times 16c \times 8c$ is considered; see Fig. 1(a). This domain is sufficient for accommodating the wake structures without wall effects and has been chosen through a domain-independence test. A 3D Cartesian coordinate system is considered with the origin located at the leading-edge of the wing. The leading-edge of the wing is situated at a distance of $5c$ from the inlet along the X-axis, and is symmetrically spanned along the Z-axis with the center of the span being located at $z = 0$. The incoming flow and the wing motion are considered along the X and Y-directions, respectively. A uniform flow condition and zero pressure gradient are imposed on the inlet boundary, and zero velocity and pressure gradients are imposed on the outlet boundary. The slip boundary condition, satisfying no-normal velocity and zero pressure-gradient, is enforced on all the side walls. The immersed boundary condition is applied on the surface of the oscillating wing. A structured mesh is chosen through a grid independence study by changing the mesh density in the near-wake region, marked by 'A' in Fig. 1(b). The result of the grid-independence study, presented in Fig. 1(c), shows a spatial resolution of $\Delta x = \Delta y = 0.045$ is sufficient to ensure converged results. A time step of 0.001 is chosen through a time-step independence study, see Fig. 1(d). The flow-solver is quantitatively validated by comparing the

time-history of C_l with the results of Han *et al.* [7] for a simultaneously pitching-plunging airfoil (see Fig. 2) and a good match is observed.

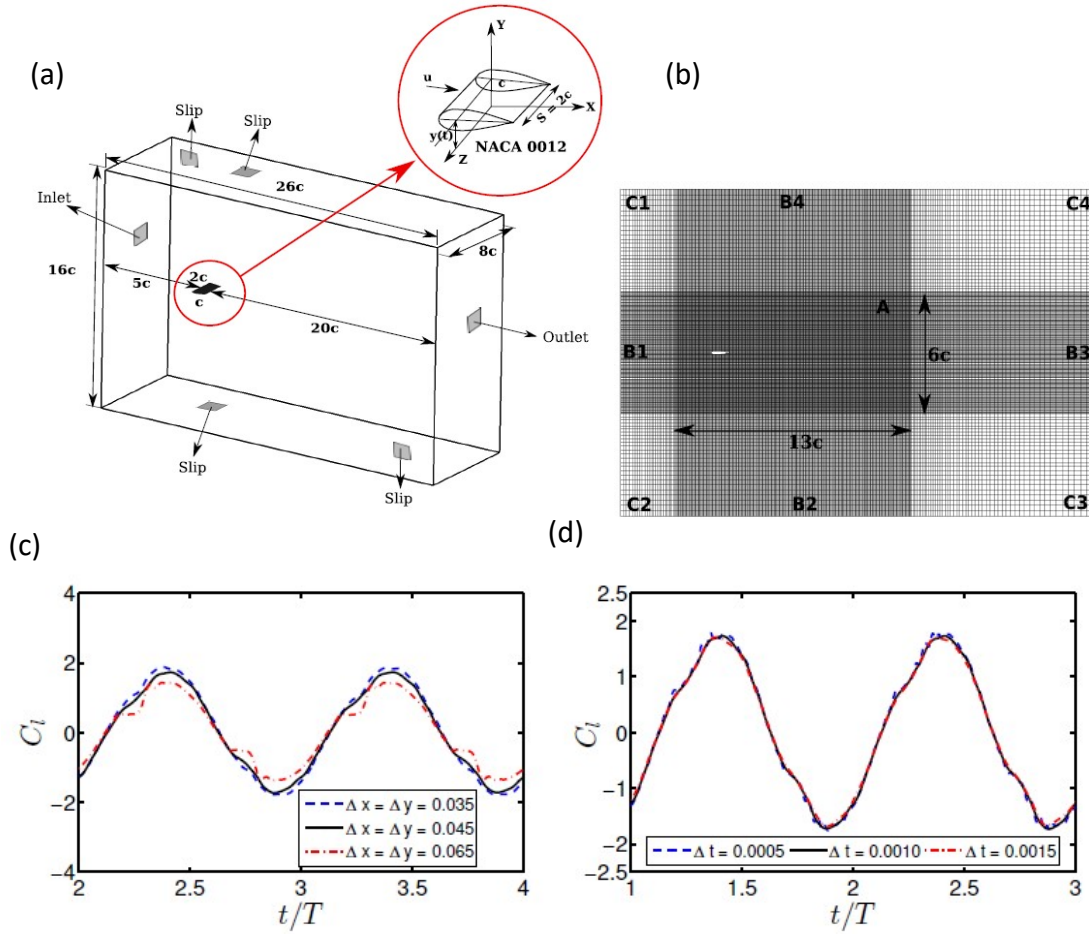


Fig. 1: (a) Computational domain; (b) mesh; (c) grid-independence result; (d) time-step independence result.

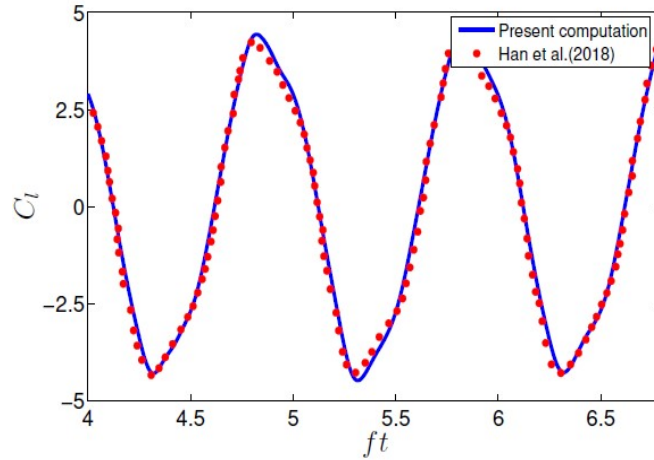


Fig. 2: Quantitative validation of the present IBM solver. Comparison of time history of lift coefficient (C_l) with the results of Han *et al.* [7] for a simultaneously pitching-plunging airfoil with $\alpha = 30^\circ$, $h = 0.5$, $\phi = 90^\circ$, $St_A = 0.6$, $Re = 200$.

Representative Results:

The 3D flow-field remains periodic up to moderately higher values of κh indicating that 3D wakes behind flapping wings are more stable in comparison to the 2D wake. The 3D periodic wakes are observed to comprise of two sets of vortex rings (VR) convecting upwards and downwards alternatively, at oblique angles about the mean horizontal axis and is designated as a ‘bifurcated wake’. As κh is gradually increased to considerably higher values, the wake is seen to lose its periodicity. The bifurcated wake pattern breaks down to an aperiodic state through complex interactions between the near-field flow structures. Figure 3 presents the typical periodic and aperiodic wake patterns (a and b) and the streamlines in the corresponding regimes (c and d). The behavior of the streamlines clearly show that contribution of the LEV and TiVs are almost negligible in the near-field interactions in the periodic regime. On the other hand, strong interactions among the LEV, TEV and TiVs are observed in the aperiodic regimes that eventually lead to the breakdown of the organized wake pattern. Despite some claims raised in the existing literature that aperiodicity and chaos do not exist in 3D flow-field, aperiodicity in the flow-field has been observed in the present study for a significantly higher value of κh as compared to the 2D cases [7]. Note that chaos and aperiodicity in 2D cases have been well established at high κh values [8]. The findings of the present study conclusively show that the qualitative nature of the dynamical transitions is very similar in 2D and 3D, though the bifurcation boundaries in the parametric plane vary. The complex interactions between the LEV, TEV and TiVs, that play a pivotal role in destroying the organization of the near-field wake, will be presented in the conference.

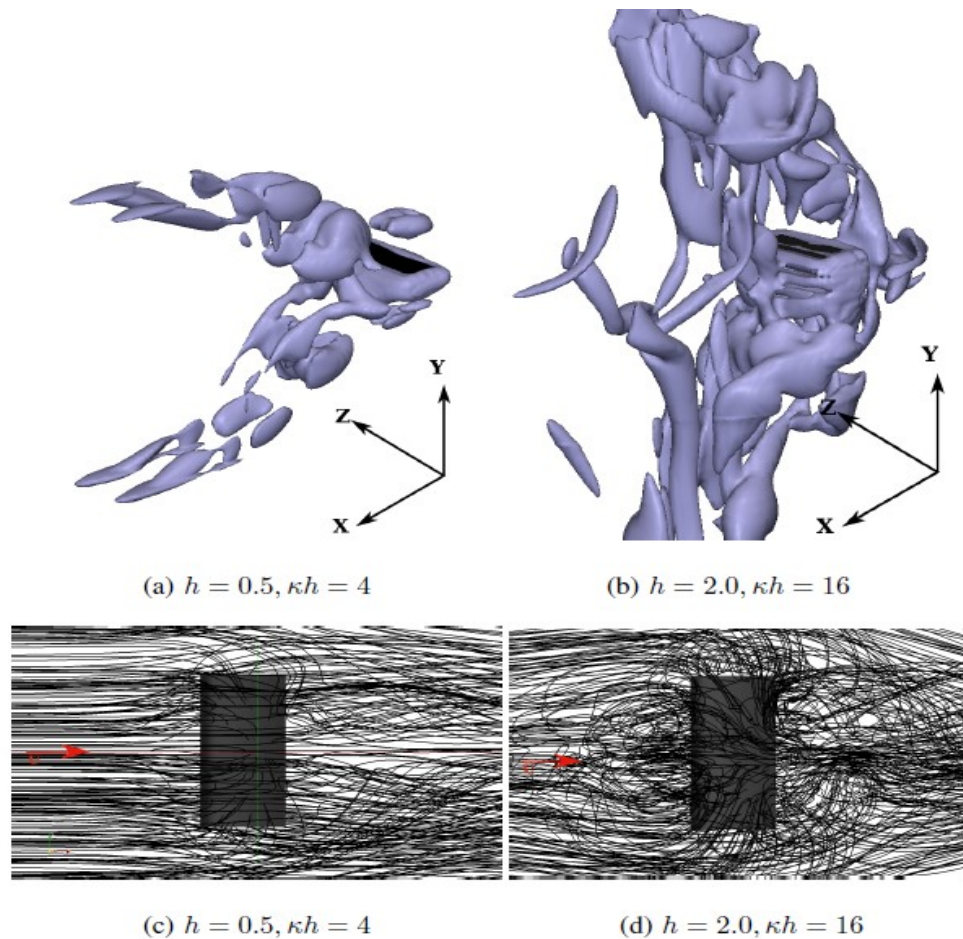


Fig. 3: Wake topology and the stream lines during periodic (a, c) and aperiodic regime (b, d) at $\kappa = 8$.

References:

1. W. Shyy, H. Aono, S. K. Chimakurthi, P. Trizila, C.-K. Kang, C. E. Cesnik, and H. Liu, "Recent progress in flapping wing aerodynamics and aeroelasticity," *Progress in Aerospace Sciences* 46, 284–327 (2010).
2. M. S. Triantafyllou, G. Triantafyllou, and D. Yue, "Hydrodynamics of fishlike swimming," *Annual Review of Fluid Mechanics* 32, 33–53 (2000).
3. W. Shyy, Y. Lian, J. Tang, D. Vieru, and H. Liu, *Aerodynamics of low Reynolds number flyers*, Vol. 22 (Cambridge University Press, 2007).
4. V. C. Sambilay Jr et al., "Interrelationships between swimming speed, caudal fin aspect ratio and body length of fishes," *Fishbyte* 8, 16–20 (1990).
5. H. Jasak, A. Jemcov, Z. Tukovic, et al., "OpenFOAM: A C++ library for complex physics simulations," in *International Workshop on Coupled Methods in Numerical Dynamics*, Vol. 1000 (IUC Dubrovnik Croatia, 2007) pp. 1–20.
6. H. Jasak, D. Rigler, and Z. Tukovic, "Design and implementation of immersed boundary method with discrete forcing approach for boundary conditions," in *11th World Congress on*

Computational Mechanics, WCCM 2014, 5th European Conference on Computational Mechanics, ECCM 2014 and 6th European Conference on Computational Fluid Dynamics, ECFD 2014 (International Center for Numerical Methods in Engineering, 2014) pp. 5319–5332.

7. J. Han, Z. Yuan, and G. Chen, "Effects of kinematic parameters on three-dimensional flapping wing at low Reynolds number," *Physics of Fluids*, 30, 081901 (2018).
8. M. R. Visbal, "High-fidelity simulation of transitional flows past a plunging airfoil", *AIAA Journal*, 47(11), 2685-2697 (2009).
9. C. Bose, and S. Sarkar, "Investigating chaotic wake dynamics past a flapping airfoil and the role of vortex interactions behind the chaotic transition", *Physics of Fluids*, 30(4), 047101 (2018).